

PAPER • OPEN ACCESS

Angular emission distribution of O 1s photoelectrons of uniaxially oriented methanol

To cite this article: L Kaiser *et al* 2020 *J. Phys. B: At. Mol. Opt. Phys.* **53** 194002

View the [article online](#) for updates and enhancements.



IOP | ebooks™

Bringing together innovative digital publishing with leading authors from the global scientific community.

Start exploring the collection—download the first chapter of every title for free.

Angular emission distribution of O 1s photoelectrons of uniaxially oriented methanol

L Kaiser¹, K Fehre¹ , N M Novikovskiy^{2,3}, J Stindl¹ , D Tsitsonis¹ ,
G Gopakumar⁴, I Unger^{4,5}, J Söderström⁴, O Björneholm⁴, M Schöffler¹,
T Jahnke¹, R Dörner¹ , F Trinter^{1,5,6,7}  and Ph V Demekhin^{2,7} 

¹ Institut für Kernphysik, Goethe-Universität, Max-von-Laue-Str. 1, 60438 Frankfurt am Main, Germany

² Institut für Physik und CINSA, Universität Kassel, Heinrich-Plett-Str. 40, 34142 Kassel, Germany

³ Institute of Physics, Southern Federal University, 344090 Rostov-on-Don, Russia

⁴ Department of Physics and Astronomy, Uppsala University, Box 516, 75120 Uppsala, Sweden

⁵ Deutsches Elektronen-Synchrotron DESY, Notkestr. 85, 22763 Hamburg, Germany

⁶ Molecular Physics, Fritz-Haber-Institut der Max-Planck-Gesellschaft, Faradayweg 4-6, 14195 Berlin, Germany

E-mail: trinter@atom.uni-frankfurt.de and demekhin@physik.uni-kassel.de

Received 24 April 2020, revised 8 June 2020

Accepted for publication 8 July 2020


Published 25 August 2020



Abstract

The angular distribution of O 1s photoelectrons emitted from uniaxially oriented methanol is studied experimentally and theoretically. We employed circularly polarized photons of an energy of $h\nu = 550$ eV for our investigations. We measured the three-dimensional photoelectron angular distributions of methanol, with the CH₃–OH axis oriented in the polarization plane, by means of cold target recoil ion momentum spectroscopy. The experimental results are interpreted by single active electron calculations performed with the single center method. A comparative theoretical study of the respective molecular-frame angular distributions of O 1s photoelectrons of CO, performed for the same photoelectron kinetic energy and for a set of different internuclear distances, allows for disentangling the role of internuclear distance and the hydrogen atoms of methanol as compared to carbon monoxide.

Keywords: photoionization, methanol, molecular-frame photoelectron angular distributions

 Supplementary material for this article is available [online](#)


(Some figures may appear in colour only in the online journal)

1. Introduction

In the emission of photoelectrons from molecules, the photoelectron's angular emission distribution in the body-fixed frame of the molecule is an exquisitely sensitive probe of molecular shape resonances [1–6], molecular structure

[2, 7–11], localization of core holes [12–16], electron correlation [3, 17–22], multi-electron processes [17, 23–26], initial electronic state [27–29], nuclear dynamics [30, 31], and allows to probe Auger decay [32–34]. Such electron angular distributions in the molecular frame of reference are typically termed MFPADs (molecular-frame photoelectron angular distributions). From a more intuitive point of view, the MFPAD arises as the outgoing photoelectron wave is multiply scattered by the molecular potential. The observed distributions depend strongly on the electron energy (i.e. the electron wavelength) and the exact shape of the molecular potential [35, 36].

⁷ Authors to whom any correspondence should be addressed.

 Original content from this work may be used under the terms of the [Creative Commons Attribution 4.0 licence](#). Any further distribution of this work must maintain attribution to the author(s) and the title of the work, journal citation and DOI.

In order to access the body-fixed molecular frame, the spatial orientation of the molecule needs to be known. In the gas phase, there are two main routes to address this experimental problem. Firstly, the molecules can be aligned actively. The field of active alignment can be partitioned further into several subsets. One approach utilizes the strong field of a laser to adiabatically align the molecule due to its polarizability. In other sets of experiments, an impulsive alignment is achieved as a defined rotation of the molecule is induced by short laser pulses. In that case, an alignment of the molecule occurs periodically after fixed time intervals, and revivals of the alignment are observable even for long times after the initial laser pulse (i.e. the alignment reoccurs, see e.g. [37, 38]). Both approaches of ‘adiabatic’ and ‘dynamic’ alignment are well reviewed, for example by Stapelfeldt and Seideman [39]. Furthermore, DC fields from multi-pole electric structures acting on molecular beams (see e.g. [40]) have been used as well, to actively align molecules. Experiments achieving an alignment by investigating molecular adsorbates on surfaces (see e.g. [41]) are also reported in the literature. The second chosen route, which is routinely employed in synchrotron-related studies, consists of an *a posteriori* measurement of the molecular orientation, and thus does not consist of an active spatial alignment of the molecule. In order for this approach to be applicable, the molecule needs to dissociate during the ionization process. If the dissociation occurs rapidly, the emission direction of the ionic fragments corresponds (e.g. for a diatomic molecule) to the direction of the molecular bond at the instant of the ionization (an assumption which is known as the so-called ‘axial recoil approximation’ [42]). This approach is typically employed in cases, where several charges are created after the primary ionization by Auger decay and is also the basis for Coulomb explosion imaging [43, 44].

It is the latter approach, i.e. the extraction of molecular orientation from measured data, which we chose for the experimental part of our present study where we make use of the power of MFPADs to probe molecular structure. For the theoretical part, we investigate by calculations, which we benchmark against our experiment on methanol, how variations in the molecular structure—such as bond length changes and addition of hydrogen atoms—influence the MFPADs. The photoelectron is released locally through core-level photoionization, and we observe the interference and scattering pattern of the emitted photoelectron wave. Due to the positive charges of the nuclei and the density distribution of electrons in a molecule, the photoelectron wave can be preferentially emitted (focused) in the direction of their neighboring atoms (for example, in diatomic molecules the photoelectron tends to an emission towards the other atom) or scattered by them [35]. These effects depend on the energy of the photoelectrons, on the respective internuclear separations, and on the nuclear charges. For instance, the MFPADs of C 1s photoelectrons of methane directly illustrate the three-dimensional molecular structure [8, 9]. In diatomic molecules, the internuclear distance has been mapped by such photoelectron interference in single-photon ionization [9, 10, 45] or strong-field ionization [11]. In summary, the emitted photoelectron wave illuminates the molecular potential from within [2].

Our present choice for studying MFPADs relates to the smallest alcohol, methanol (CH₃OH). Methanol is used not only as a solvent, but it is also used in fuels and in direct-methanol fuel cells, and can have potential future applications in energy storage. Methanol has also been observed in space in relation to certain star-forming regions [46]. Although many coincidence experiments on methanol have been performed using strong-field ionization [47–53], ion impact ionization [54], VUV [55] and EUV [56] photoionization, only a limited number of soft x-ray coincidence studies on methanol exist [57–59]. In the present work, we examine the MFPADs of O 1s photoelectrons approximately 8.5 eV above the oxygen K-threshold. Although the orientation of molecules in the gas phase is random, we are able to post-select cases where the molecular CH₃–OH axis is oriented within the polarization plane (i.e., the plane normal to the Poynting vector) of the circularly polarized photons, using the relative momenta of the fragment ions. In contrast to linear polarization, circularly polarized light (CPL) does not introduce a preferable direction of emission in the polarization plane, but rather imprints a sense of its rotation on the emitted photoelectron wave. Therefore, using circular polarization has an advantage to sense the molecular structure itself. In the industrially relevant process of catalytic hydrogenation to produce methanol, carbon monoxide is the precursor. The structures of CO and CH₃OH have their central C–O bond in common and differ only in the attached hydrogen atoms and in the C–O bond length. The similarity between these molecules motivated us to perform an extended theoretical study of the respective MFPAD of CO to compare the methanol data with.

2. Methods

The experiments were carried out at the soft x-ray beamline P04 of the synchrotron PETRA III (DESY, Hamburg, Germany) [60] in 40-bunch timing mode (bunch spacing 192 ns), using circularly polarized photons of 550 eV photon energy generated by its 5 m long APPLE-2 undulator. We used the permanently installed COLTRIMS (cold target recoil ion momentum spectroscopy) reaction microscope [61–63] for our studies. The methanol molecules were provided as a supersonic gas jet, which passed two skimmers (300 μm diameter) and was crossed with the photon beam at right angle. The methanol reservoir was heated to 316 K (vapor pressure of approximately 400 mbar), and by also heating up the gas line to 319 K and the gas nozzle of 100 μm diameter to 328 K (vapor pressure of approximately 680 mbar), we achieved suitable conditions at the supersonic expansion of the vapor. The COLTRIMS spectrometer employed consisted of an ion arm of 7 cm length and an electron arm of 15 cm length. Both were equipped with a micro-channel plate detector (active area of 80 mm diameter) with hexagonal delay-line position readout [64, 65]. For the ion detection, a funnel micro-channel plate [66] was used to achieve high coincidence detection efficiency. Electrons and ions were guided by homogeneous electric (21.9 V cm⁻¹) and magnetic fields (6.3 G) onto the two time- and position-sensitive detectors. These fields were selected such that 4π collection solid angle for

electrons and ions has been achieved for electrons up to 30 eV kinetic energy and molecular fragmentation with a kinetic energy release up to 20 eV. From the times-of-flight and the positions-of-impact, the three-dimensional momentum vectors of all charged fragments of the photoreaction were retrieved. In addition, the time-of-flight measurement allowed identifying different breakup channels. We focus on the case of O 1s-photoionization followed by Auger decay here, and a fragmentation of the molecule into $\text{CH}_3^+/\text{OH}^+$. These fragments were detected in coincidence with the O 1s photoelectrons of 8.5 eV kinetic energy. The corresponding events were selected by gating on the time-of-flight coincidence of the two photoions and the photoelectron and on the photoelectron kinetic energy.

For CPL and within the electric dipole approximation, the MFPAD of a fixed-in-space (i.e. spatially aligned) molecule is given by the following differential photoionization cross section:

$$\frac{d\sigma^{\pm 1}}{d\Omega}(\alpha\beta\gamma, \theta'\varphi') = \left| \sum_{\ell m k} (-i)^\ell D_{k\pm 1}^1(\alpha\beta\gamma) A_{\ell m k} Y_{\ell m}(\theta'\varphi') \right|^2, \quad (1)$$

here, ± 1 stand for the positive and negative helicity of the CPL; D stands for the Wigner rotation matrix, which depends on the three molecular-orientation Euler angles $\{\alpha, \beta, \gamma\}$; Y stands for the spherical harmonics; and θ', φ' are the photoelectron emission angles in the molecular frame of reference. The electron dynamics of the photoionization process are imprinted on the MFPAD in equation (1) through the dipole transition amplitudes $A_{\ell m k}$ for the emission of the partial photoelectron continuum waves $|\varepsilon \ell m\rangle$ [67] with given energy and angular momentum quantum numbers via the absorption of a photon of polarization k . In our modeling, those amplitudes were computed by using the stationary single center (SC) method [68, 69], which provides an accurate theoretical description of the angle-resolved photoemission spectra of molecules [70–84]. The calculations were performed in the frozen-core Hartree–Fock approximation at the equilibrium internuclear geometry for methanol and at different internuclear separations for carbon monoxide. The SC expansions of the occupied and continuum orbitals with respect to the central point between the C and O atoms were restricted to the partial harmonics with $\ell, |m| \leq 49$ and $\ell, |m| \leq 29$, respectively. Because of the axial symmetry of the CPL, the orientation angle γ , which describes the rotation around the light propagation direction (the laboratory z -axis), is irrelevant. In order to put the molecular z' -axis (chosen along the C–O bond) in the polarization plane (the laboratory xy -plane), the orientation angle β is set to 90° . Finally, since only the C–O bond of methanol was fixed in space in the experiment, the computed MFPADs have been integrated over the orientation angle α , which describes the rotation around the molecular z' -axis, and the emission angle φ' must be reset accordingly.

3. Results and discussion

We start our discussion with the theoretical results obtained for carbon monoxide. To confirm the reliability of the

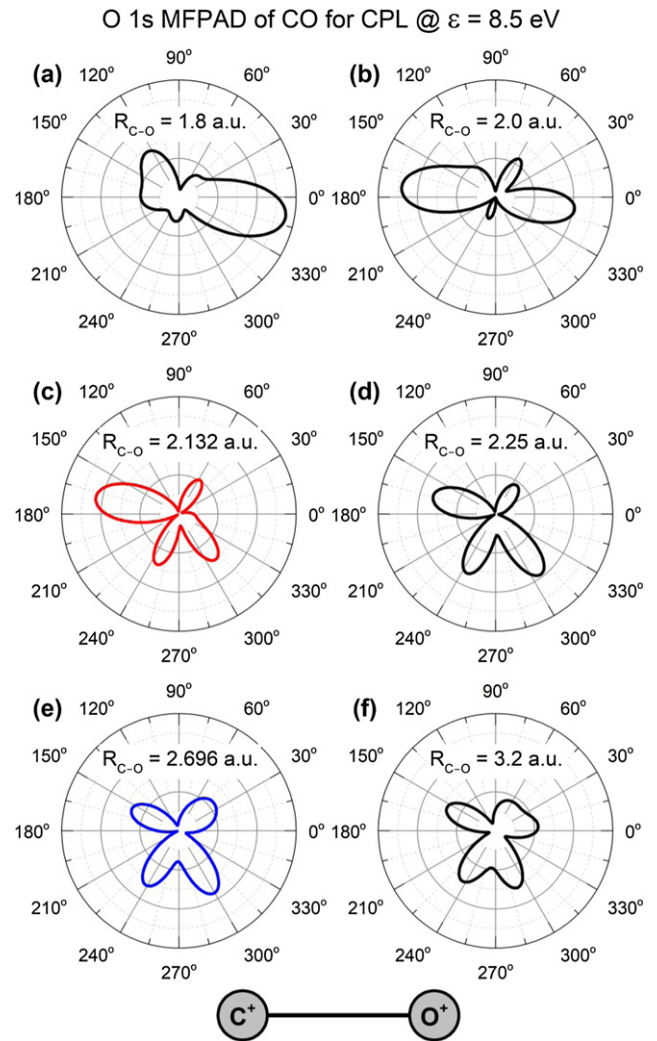


Figure 1. Predicted angular emission distributions of O 1s photoelectrons of CO, computed for CPL with negative helicity and a photoelectron kinetic energy of 8.5 eV at different internuclear distances, as indicated in each panel. The light propagates out of the page plane (the polarization plane), and the photoelectrons are emitted within this plane. The molecule is oriented to lie within the polarization plane with the oxygen ion pointing to the right, as indicated at the bottom. The internuclear distances in panels (c) and (e) correspond to the equilibrium distances of CO and CH_3OH , respectively.

present theoretical approach, we firstly reproduced available experimental MFPADs of O 1s photoelectrons from reference [25] (see figure 15 in reference [25]), which were measured for linearly polarized light and somewhat different kinetic energy of 11.7 eV. The agreement is excellent (not shown here for brevity). In the next step, MFPADs of O 1s photoelectrons of CO were computed for left-handed CPL and a kinetic energy of 8.5 eV (as in the present experiment for methanol). The calculations have been performed for different internuclear separations, from somewhat smaller than the equilibrium internuclear distance of carbon monoxide ($R_{\text{C-O}} = 2.132$ a.u. [85]) to somewhat larger than that of methanol ($R_{\text{CH}_3\text{-OH}} = 2.696$ a.u. [86]). The results are summarized in figure 1. As one can see from this figure, the lobe, which points towards the C^+ ion, develops dramatically with the increase of the internuclear

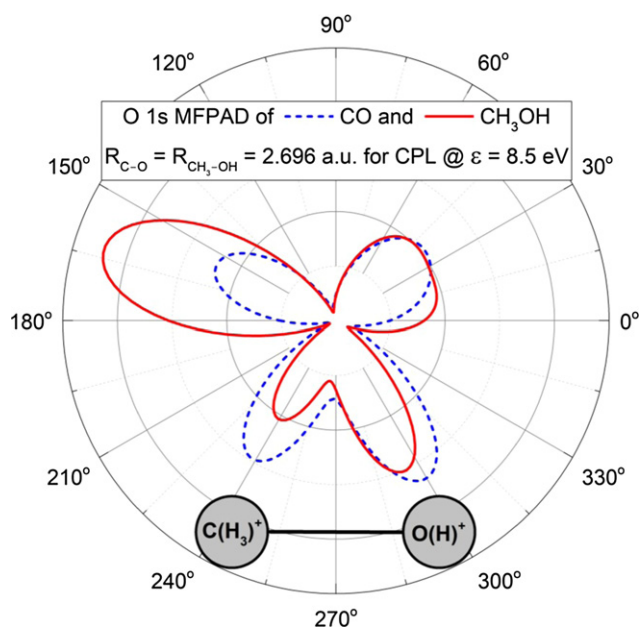


Figure 2. Comparison of the MFPADs of O 1s photoelectrons of CO and CH₃OH, computed for CPL with negative helicity and photoelectron kinetic energy of 8.5 eV at the equilibrium internuclear distance $R_{C-O} = R_{CH_3-OH} = 2.696$ a.u. of CH₃OH. The MFPAD of CO is the same as in figure 1(e). The light propagates out of the page plane (the polarization plane), and the photoelectrons are emitted within this plane. The molecules are oriented in the polarization plane with the O⁺ or OH⁺ ions pointing to the right, as indicated at the bottom.

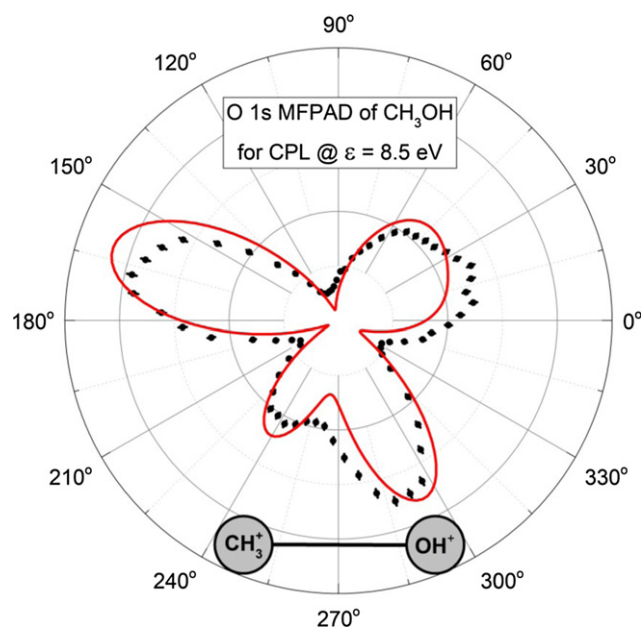


Figure 3. Comparison of the measured (solid circles with error bars) and computed (red curve) two-dimensional MFPADs of O 1s photoelectrons of methanol, obtained for CPL with negative helicity and photoelectron kinetic energy of 8.5 eV. The light propagates out of the page plane (the polarization plane). The MFPADs include all photoelectrons, which fall in the opening angle of $\pm 12^\circ$, and the molecular CH₃-OH axis is oriented within the opening angle of $\pm 15^\circ$, both around the polarization plane. The OH⁺ ion points to the right, as indicated at the bottom.

distance. At $R_{C-O} = 1.8$ a.u. in figure 1(a), it is somewhat suppressed, and for larger distance of $R_{C-O} = 2.0$ a.u. in figure 1(b), becomes strongly enhanced. The computed MFPAD shows its well-known form at the equilibrium internuclear distance $R_{C-O} = 2.132$ a.u. of CO in figure 1(c) (red curve). Further on, in figures 1(d)–(f), the main lobe continuously shrinks with the increase of the internuclear distance across the equilibrium distance $R_{C-O} = 2.696$ a.u. of CH₃OH (blue curve in figure 1(e)). Not surprisingly increasing the bond length at fixed photoelectron wavelength results in a similar trend as decreasing the photoelectron wavelength at a given bond length [17, 87].

In the next step, we inspected the MFPADs of carbon monoxide using the equilibrium distance $R_{C-O} = 2.696$ a.u. of CH₃OH. Starting from this model system, we then built the methanol molecule by introducing one by one additional hydrogen atoms, first on the oxygen site, and then on the carbon site. For brevity, we compare in figure 2 the final result for the complete methanol molecule with all four hydrogen atoms to that computed for CO using an internuclear distance of $R_{C-O} = 2.696$ a.u. The full account of calculations can be found in figure S1 of the supplemental material, which can be found online at <https://stacks.iop.org/JPB/53/194002/mmedia>. We observe that introducing hydrogen atoms systematically increases the main lobe pointing towards the carbon site in the computed MFPAD, as compared to the MFPAD of CO at this internuclear distance (depicted in figure 1(e)). Figure 2 illustrates the strong impact of the hydrogen atoms on the computed

MFPAD. In particular, they recover the main lobe pointing towards the CH₃⁺ ion, as compared to the MFPAD of CO from figure 1(e) (shown here for reference by the blue dashed curve), to the form of the MFPAD of CO from figure 1(c) obtained for its equilibrium internuclear distance $R_{C-O} = 2.132$ a.u. Detailed interpretation of this effect requires an accurate analysis of multiple-scattering effects of photoelectron waves in the ionic potential of methanol, which is a cumbersome task. However, we suggest that the focusing effect plays a dominant role in this case. In particular, photoelectron waves emitted in the direction of the carbon atom experience a large uncompensated positive charge of its nucleus, which works as a lens and focuses photoelectron waves in this direction. In methanol, the positive charge of each additional proton of the methyl group (CH₃) introduces its own focusing, enhancing thereby the effect of the carbon nucleus alone in CO. The CPL additionally imprints its rotational sense on the photoelectron waves, causing thereby a slight clockwise rotation of the emission distribution along the rotation of the electric field vector.

The measured results for methanol are compared to our theoretical findings in figures 3 and 4. Figure 3 illustrates an excellent agreement between the computed and measured dipole-plane MFPADs of methanol (note that the depicted data accounts for opening angles of $\pm 12^\circ$ and $\pm 15^\circ$ around the polarization plane, respectively, for the photoelectron and the CH₃-OH axis, as in the experiment). A similarly excellent agreement between the modeling and the experiment is also evident from figure 4. It compares the full three-dimensional

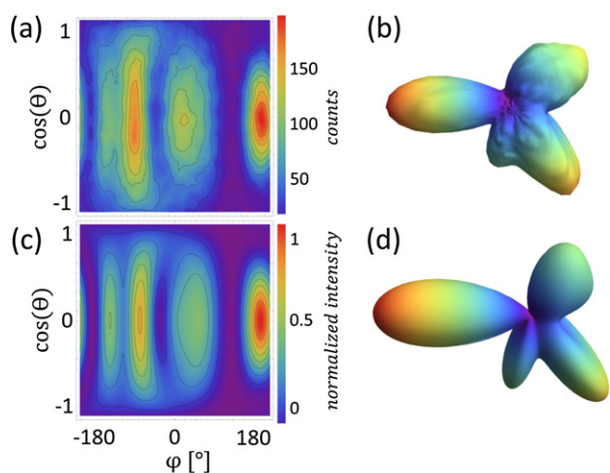


Figure 4. Comparison of the measured ((a) and (b)) and computed ((c) and (d)) three-dimensional MFPADs of O 1s photoelectrons of methanol, obtained for CPL with negative helicity and photoelectron kinetic energy of 8.5 eV. In panels (b) and (d), the light propagates out of the page plane (the polarization plane), and the molecule is oriented horizontally with the OH⁺ ion pointing to the right. The data include the CH₃⁺/OH⁺ breakups (molecular axis orientations), which fall in the opening angle of $\pm 15^\circ$ around the polarization plane. Panels (a) and (c) show the same three-dimensional MFPADs in a color-map representation as functions of the polar and azimuthal angles. In this representation, the light propagation direction points from $\cos(\theta) = -1$ to $\cos(\theta) = 1$.

MFPADs of methanol in two representations: via a color-map as a function of the spherical angles (panels (a) and (c) in the left column) and as three-dimensional figures where the angular variation of the photoelectron yield is encoded in the distance of the surface from the origin (panels (b) and (d) in the right column).

4. Conclusions

We investigated angular distributions of O 1s photoelectrons emitted from uniaxially oriented methanol molecules. The molecular CH₃–OH axis has been fixed in the polarization plane of the circularly polarized ionizing radiation. The experimental angular distributions have been recorded using the COLTRIMS technique at the synchrotron radiation facility PETRA III (DESY). The measured three-dimensional photoelectron momentum distributions of methanol are in a very good agreement with those computed by the SC method and code. In order to understand the findings in more detail, we calculated O 1s photoelectrons of carbon monoxide at the same photoelectron kinetic energy. These two molecules have the following main differences: firstly, the C–O bond of methanol is about 25% longer than that of CO. Enlarging this distance results in a considerable suppression of the main lobe pointing towards the carbon atom in the computed MFPAD of CO. Secondly, methanol has four additional hydrogen atoms as compared to CO. The additional protons of the methyl group seem to enlarge the focusing effect of the carbon nucleus and recover thereby the corresponding main lobe in the computed distribution to its experimentally observed form.

Acknowledgments

We acknowledge DESY (Hamburg, Germany), a member of the Helmholtz Association HGF, for the provision of experimental facilities. Parts of this research were carried out at PETRA III within the project I-20180746-EC, and we would like to thank the staff of beamline P04 for excellent support during the beam time. This research was supported in part through the Maxwell computational resources operated at DESY. The experiments were supported by Deutsche Forschungsgemeinschaft via Sonderforschungsbereich 1319 (ELCH) and by the Bundesministerium für Bildung und Forschung (BMBF, Federal Ministry of Education and Research). The theoretical work was supported by the DFG Project DE 2366/1-2. KF acknowledges support by the German National Merit Foundation. GG, IU, JS, and OB acknowledge support from the Swedish Research Council project 2017-04162.

ORCID iDs

K Fehre [ID](https://orcid.org/0000-0003-2519-5564) <https://orcid.org/0000-0003-2519-5564>
 J Stindl [ID](https://orcid.org/0000-0002-5041-2404) <https://orcid.org/0000-0002-5041-2404>
 D Tsitsonis [ID](https://orcid.org/0000-0002-8748-6677) <https://orcid.org/0000-0002-8748-6677>
 R Dörner [ID](https://orcid.org/0000-0002-3728-4268) <https://orcid.org/0000-0002-3728-4268>
 F Trinter [ID](https://orcid.org/0000-0002-0891-9180) <https://orcid.org/0000-0002-0891-9180>
 Ph V Demekhin [ID](https://orcid.org/0000-0001-9797-6648) <https://orcid.org/0000-0001-9797-6648>

References

- [1] Shigemasa E, Adachi J, Oura M and Yagishita A 1995 *Phys. Rev. Lett.* **74** 359
- [2] Landers A et al 2001 *Phys. Rev. Lett.* **87** 013002
- [3] Cherepkov N A, Semenov S K, Hikosaka Y, Ito K, Motoki S and Yagishita A 2000 *Phys. Rev. Lett.* **84** 250
- [4] Shigemasa E, Adachi J, Soejima K, Watanabe N, Yagishita A and Cherepkov N A 1998 *Phys. Rev. Lett.* **80** 1622
- [5] Jahnke T et al 2002 *Phys. Rev. Lett.* **88** 073002
- [6] De Fanis A et al 2002 *Phys. Rev. Lett.* **89** 023006
- [7] Williams J B et al 2012 *Phys. Rev. Lett.* **108** 233002
- [8] Williams J B et al 2012 *J. Phys. B: At. Mol. Opt. Phys.* **45** 194003
- [9] Kreidi K et al 2008 *Phys. Rev. Lett.* **100** 133005
- [10] Schöffler M S et al 2008 *Phys. Rev. A* **78** 013414
- [11] Kunitski M et al 2019 *Nat. Commun.* **10** 1
- [12] Schöffler M S et al 2008 *Science* **320** 920
- [13] Kreidi K et al 2008 *J. Phys. B: At. Mol. Opt. Phys.* **41** 101002
- [14] McCurdy C W et al 2017 *Phys. Rev. A* **95** 011401
- [15] Saito N et al 2003 *J. Phys. B: At. Mol. Opt. Phys.* **36** L25
- [16] Zimmermann B et al 2008 *Nat. Phys.* **4** 649
- [17] Martin F et al 2007 *Science* **315** 629
- [18] Waitz M et al 2017 *Nat. Commun.* **8** 2266
- [19] Waitz M et al 2016 *Phys. Rev. Lett.* **116** 043001
- [20] Waitz M et al 2016 *Phys. Rev. Lett.* **117** 083002
- [21] Liu X-J et al 2008 *Phys. Rev. Lett.* **101** 023001
- [22] Liu X-J et al 2008 *Phys. Rev. Lett.* **101** 083001
- [23] Lebech M, Houver J C, Dowek D and Lucchese R R 2006 *Phys. Rev. Lett.* **96** 073001
- [24] Golovin A V, Heiser F, Quayle C J K, Morin P, Simon M, Gessner O, Guyon P-M and Becker U 1997 *Phys. Rev. Lett.* **79** 4554

- [25] Jahnke T *et al* 2004 *J. Electron Spectrosc. Relat. Phenom.* **141** 229
- [26] Akoury D *et al* 2007 *Science* **318** 949
- [27] Arasaki Y, Takatsuka K, Wang K and McKoy V 2010 *J. Chem. Phys.* **132** 124307
- [28] Hockett P, Bisgaard C Z, Clarkin O J and Stolow A 2011 *Nat. Phys.* **7** 612
- [29] Mignolet B, Levine R D and Remacle F 2012 *Phys. Rev. A* **86** 053429
- [30] Kircher M *et al* 2019 *Phys. Rev. Lett.* **123** 243201
- [31] Sturm F P *et al* 2009 *Phys. Rev. A* **80** 032506
- [32] Cherepkov N A *et al* 2009 *Phys. Rev. A* **80** 051404
- [33] Semenov S K *et al* 2010 *Phys. Rev. A* **81** 043426
- [34] Weber T *et al* 2003 *Phys. Rev. Lett.* **90** 153003
- [35] Söderström J *et al* 2012 *Phys. Rev. Lett.* **108** 193005
- [36] Travnikova O *et al* 2019 *J. Phys. Chem. A* **123** 7619
- [37] Wu J *et al* 2011 *Phys. Rev. A* **83** 061403
- [38] Wu J, Magrakvelidze M, Vredenburg A, Schmidt L P H, Jahnke T, Czasch A, Dörner R and Thumm U 2013 *Phys. Rev. Lett.* **110** 033005
- [39] Stapelfeldt H and Seideman T 2003 *Rev. Mod. Phys.* **75** 543
- [40] Rakitzis T P, van den Brom A J and Janssen M H M 2004 *Science* **303** 1852
- [41] Lablanquie P *et al* 1989 *Phys. Rev. A* **40** 5673
- [42] Zare R N 1972 *Mol. Photochem.* **4** 1
- [43] Vager Z, Naaman R and Kanter E P 1989 *Science* **244** 426
- [44] Pitzer M *et al* 2013 *Science* **341** 1096
- [45] Fukuzawa H *et al* 2019 *J. Chem. Phys.* **151** 104302
- [46] Pilling S, Neves R, Santos A C F and Boechat-Roberly H M 2007 *Astron. Astrophys.* **464** 393
- [47] Okino T, Furukawa Y, Liu P, Ichikawa T, Itakura R, Hoshina K, Yamanouchi K and Nakano H 2006 *Chem. Phys. Lett.* **419** 223
- [48] Okino T, Furukawa Y, Liu P, Ichikawa T, Itakura R, Hoshina K, Yamanouchi K and Nakano H 2006 *Chem. Phys. Lett.* **423** 220
- [49] Okino T, Furukawa Y, Liu P, Ichikawa T, Itakura R, Hoshina K, Yamanouchi K and Nakano H 2006 *J. Phys. B: At. Mol. Opt. Phys.* **39** S515
- [50] Itakura R, Liu P, Furukawa Y, Okino T, Yamanouchi K and Nakano H 2007 *J. Chem. Phys.* **127** 104306
- [51] Xu H, Marceau C, Nakai K, Okino T, Chin S-L and Yamanouchi K 2010 *J. Chem. Phys.* **133** 071103
- [52] Xu H, Okino T, Kudou T, Yamanouchi K, Roither S, Kitzler M, Baltuska A and Chin S-L 2012 *J. Phys. Chem. A* **116** 2686
- [53] Fukahori S, Nakano M, Yamanouchi K and Itakura R 2017 *Chem. Phys. Lett.* **672** 7
- [54] De S, Roy A, Rajput J, Ghosh P N and Safvan C P 2008 *Int. J. Mass Spectrom.* **276** 43
- [55] Borkar S, Sztaray B and Bodi A 2011 *Phys. Chem. Chem. Phys.* **13** 13009
- [56] Luzon I, Jagtap K, Livshits E, Lioubashevski O, Baer R and Strasser D 2017 *Phys. Chem. Chem. Phys.* **19** 13488
- [57] Hempelmann A, Piancastelli M N, Heiser F, Gessner O, Rüdell A and Becker U 1999 *J. Phys. B: At. Mol. Opt. Phys.* **32** 2677
- [58] Pilling S, Boechat-Roberly H M, Santos A C F and de Souza G G B 2007 *J. Electron Spectrosc. Relat. Phenom.* **155** 70
- [59] Kivimäki A, Strahlman C, Richter R and Sankari R 2018 *J. Phys. Chem. A* **122** 224
- [60] Viefhaus J, Scholz F, Deinert S, Glaser L, Ilchen M, Seltmann J, Walter P and Siewert F 2013 *Nucl. Instrum. Methods Phys. Res. A* **710** 151
- [61] Dörner R, Mergel V, Jagutzki O, Spielberger L, Ullrich J, Moshhammer R and Schmidt-Böcking H 2000 *Phys. Rep.* **330** 95
- [62] Ullrich J, Moshhammer R, Dorn A, Dörner R, Schmidt L P H and Schmidt-Böcking H 2003 *Rep. Prog. Phys.* **66** 1463
- [63] Jahnke T *et al* 2011 *J. Electron Spectrosc. Relat. Phenom.* **183** 48
- [64] Jagutzki O, Mergel V, Ullmann-Pfleger K, Spielberger L, Spillmann U, Dörner R and Schmidt-Böcking H 2002 *Nucl. Instrum. Methods Phys. Res. A* **477** 244
- [65] Jagutzki O, Lapington J S, Worth L B C, Spillman U, Mergel V and Schmidt-Böcking H 2002 *Nucl. Instrum. Methods Phys. Res. A* **477** 256
- [66] Fehre K *et al* 2018 *Rev. Sci. Instrum.* **89** 045112
- [67] Cherepkov N A 1981 *J. Phys. B: At. Mol. Opt. Phys.* **14** 2165
- [68] Demekhin P V, Ehresmann A and Sukhorukov V L 2011 *J. Chem. Phys.* **134** 024113
- [69] Galitskiy S A, Artemyev A N, Jänkälä K, Lagutin B M and Demekhin P V 2015 *J. Chem. Phys.* **142** 034306
- [70] Demekhin P V, Petrov I D, Sukhorukov V L, Kielich W, Reiss P, Hentges R, Haar I, Schmoranzler H and Ehresmann A 2009 *Phys. Rev. A* **80** 063425
- Demekhin P V, Petrov I D, Sukhorukov V L, Kielich W, Reiss P, Hentges R, Haar I, Schmoranzler H and Ehresmann A 2010 *Phys. Rev. A* **81** 069902
- [71] Demekhin P V, Petrov I D, Tanaka T, Hoshino M, Tanaka H, Ueda K, Kielich W and Ehresmann A 2010 *J. Phys. B: At. Mol. Opt. Phys.* **43** 065102
- [72] Demekhin P V, Petrov I D, Sukhorukov V L, Kielich W, Knie A, Schmoranzler H and Ehresmann A 2010 *Phys. Rev. Lett.* **104** 243001
- [73] Demekhin P V, Petrov I D, Sukhorukov V L, Kielich W, Knie A, Schmoranzler H and Ehresmann A 2010 *J. Phys. B: At. Mol. Opt. Phys.* **43** 165103
- [74] Knie A *et al* 2014 *Phys. Rev. A* **90** 013416
- [75] Antonsson E, Patanen M, Nicolas C, Benkoula S, Neville J J, Sukhorukov V L, Bozek J D, Demekhin P V and Miron C 2015 *Phys. Rev. A* **92** 042506
- [76] Sann H *et al* 2016 *Phys. Rev. Lett.* **117** 263001
- [77] Knie A, Patanen M, Hans A, Petrov I D, Bozek J D, Ehresmann A and Demekhin P V 2016 *Phys. Rev. Lett.* **116** 193002
- [78] Nandi S, Nicolas C, Artemyev A N, Novikovskiy N M, Miron C, Bozek J D and Demekhin P V 2017 *Phys. Rev. A* **96** 052501
- [79] Ilchen M *et al* 2017 *Phys. Rev. A* **95** 053423
- [80] Tia M *et al* 2017 *J. Phys. Chem. Lett.* **8** 2780
- [81] Mhamdi A *et al* 2018 *Phys. Rev. Lett.* **121** 243002
- [82] Mhamdi A *et al* 2018 *Phys. Rev. A* **97** 053407
- [83] Mhamdi A, Rist J, Havermeier T, Dörner R, Jahnke T and Demekhin P V 2020 *Phys. Rev. A* **101** 023404
- [84] Hartmann G *et al* 2019 *Phys. Rev. Lett.* **123** 043202
- [85] Huber K P and Herzberg G 1979 *Molecular Spectra and Molecular Structure. IV. Constants of Diatomic Molecules* (Princeton, NJ: Van Nostrand-Reinhold)
- [86] Venkateswarlu P and Gordy W 1955 *J. Chem. Phys.* **23** 1200
- [87] Kushawaha R K, Patanen M, Guillemin R, Journel L, Miron C, Simon M, Piancastelli M N, Skates C and Declava P 2013 *Proc. Natl Acad. Sci. USA* **110** 15201